Further contributions of the Thomas double-scattering mechanism to electron capture in the second Born approximation

Steven Alston
Physics Department, Pennsylvania State University, Wilkes-Barre Campus, Lehman, Pennsylvania 18627

(Received 26 May 1988)

The double-scattering mechanism of Thomas represents the dominant means in an ion-atom collision at high velocities for the electron-projectile subsystem to rid itself of its large internal kinetic energy and thus allow the electron to be captured. The plane-wave second Born approximation to the single-electron capture amplitude calculated in a linearized-propagator approximation gives the lowest-order quantum estimate of the Thomas mechanism by employing initial and final bound-state momentum values around the center of these distributions along with a neglect of the electronic part of the momentum transfer in the two collisions of the mechanism. It is shown that additional contributions to the amplitude deriving from values of the bound-state momentum in the wings of the distributions are non-negligible and in fact explain the large differences found between exact and linearized-propagator approximation results. Consequently, the second Born approximation is seen to suffer from the same problem as does the first Born approximation, namely, too dominant a contribution of the large bound-state momentum components.

I. INTRODUCTION

The plane-wave second Born approximation to the single-electron capture amplitude has been analyzed in great depth, notably in connection with second-order singularities of which the most well known is the Thomas peak[1,2] at forward-scattering angles. Starting with the full amplitude including the internuclear potential, one can show to the order of the electron mass over heavy-particle masses that the sum of all the internuclear terms in the amplitude gives a *zero* contribution in the forward scattering directions.[3] The remaining part of the amplitude, which includes only electronic-nuclear potentials (hereafter denoted $B2$), is further known to provide the lowest-order quantum representation of the double-scattering mechanism of Thomas which dominates in the near forward-angle region.[1,2] Extensive calculations have appeared involving capture to and from both the ground and excited states in this angular region.[4] Away from the forward angles, additional double-scattering mechanisms have been isolated in the full amplitude by critical-angle analyses.[5] Finally, exact numerical calculations of the amplitude have been reported for proton-hydrogen,[6–10] proton-helium,[11] and other[11] collisions. In this article, a new approximate but analytic evaluation of the amplitude is compared with the exact numerical one in order to understand better the poor agreement of the second Born approximation with experiment.

Since the Thomas mechanism involves two scatterings of the electron, first with the projectile and then with the target nucleus, it is natural that the second Born approximation should apply to the process, as was first shown by Drisko.[2] When the $B2$ amplitude is evaluated by (1) neglecting terms in the free Green's-function quadratic in the bound-state momentum variables and (2) disregarding electronic contributions to the momentum transfers in the two collisions, a so-called linearized-propagator approximation (LPA) to the exact amplitude is obtained.[4] The essence of this approximation is to evaluate the amplitude at bound-state momentum values (in a.u.) of the order of or less than the projectile and target-nuclear charges Z_P and Z_T, ostensibly obviating any reliance on the much less likely large momentum components of the bound states that are necessary in the first Born approximation.[12]

The LPA, however, models the exact differential cross sections well only in a very limited angular region centered about the classical Thomas peak located at 0.47 mrad for proton impact. This paper considers additional contributions to the amplitude which are derived from certain large, bound-state momentum values and calculated through the use of a multiple-peaking approximation (MPA). The resulting approximate amplitude is seen to reproduce well the exact one over all forward angles. Graphical and tabular comparisons of the LPA, MPA, and exact $B2$ cross sections are presented showing the good agreement of the latter two.

Use of the MPA leads to a very simple closed-form expression for the $B2$ amplitude for $1s \rightarrow 1s$ capture. In contrast to the first-Born cross section[12] which shows an impact-velocity dependence of v^{-1} relative to that of the LPA, some terms in the MPA amplitude contain an extra $(\ln v)/v$ dependence which leads to a *slower* convergence toward the well-known v^{-11} velocity dependence of the $B2$ total cross section which appears in the exact calculations. Preliminary results of the present work have appeared elsewhere.[13] In the following discussion, atomic units ($m = \hbar = e = 1$) are employed.

Consider a target system consisting of an active electron and a target ion of mass M_T including nucleus plus nonactive electrons. The second Born approximation to the exact amplitude representing the transfer of the active electron from the target system to the projectile ion of mass M_P at the total system energy E is given in

 ©1988 The American Physical Society

distorted-wave form by[14]

$$A_{B2}(E)=\langle X_f|V_{Pe}|\Phi_i\rangle=\langle\Phi_f|V_{Te}|X_i\rangle , \quad (1.1)$$

where the distorted-wave states are defined as

$$|X_i\rangle=[1+G_0^+(E)V_{Pe}]|\Phi_i\rangle , \quad (1.2a)$$

$$\langle X_f|=\{[1+G_0^-(E)V_{Te}]|\Phi_f\rangle\}^\dagger , \quad (1.2b)$$

with the asymptotic scattering wave functions

$$\langle\mathbf{R}_T,\mathbf{r}_T|\Phi_i\rangle=\exp(i\mathbf{K}_i\cdot\mathbf{R}_T)\phi_i(\mathbf{r}_T) ,$$

$$\langle\mathbf{R}_P,\mathbf{r}_P|\Phi_f\rangle=\exp(i\mathbf{K}_f\cdot\mathbf{R}_P)\phi_f(\mathbf{r}_P) .$$

Only that part of the full amplitude containing electronic-nuclear potentials is considered here.[1] The coordinate variables $\mathbf{r}_T,\mathbf{r}_P$ define the electron's position relative to the target-ion center-of-mass and projectile nucleus, respectively; $\mathbf{R}_T$ defines the projectile's position relative to the target-system center of mass; and $\mathbf{R}_P$ defines the target-ion position relative to the electron-projectile-nucleus center of mass. The initial (final) bound-state wave function is $\phi_i(\phi_f)$ and the initial (final) heavy-particle wave vector is $\mathbf{K}_i(\mathbf{K}_f)$.

The free Green operator $G_0^+(E)=(E-H_0+i\eta)^{-1}$ is defined in terms of the full three-body kinetic energy operator in the center-of-mass system H_0 with η denoting an infinitesimal quantity. The electron-projectile potential is given by $V_{Pe}(r_P)=-Z_P/r_P$ and the electron-target ion potential has the limiting forms

$$V_{Te}(r_T)\sim -Z_a/r_T \quad \text{as } r_T\to\infty , \quad (1.3a)$$

$$\sim -Z_s/r_T \quad \text{as } r_T\to 0 . \quad (1.3b)$$

The asymptotic charge of the target ion is denoted by Z_a. The shielding of the target nucleus of charge Z_T by all of the nonactive electrons leads to the value Z_a, and for neutral targets Z_a is unity. The inner part of V_{Te}, however, is modeled by a scaled-Coulomb potential of charge Z_s which is close to Z_T. For the numerical calculations presented in the following Eq. (1.3b) is used; Eq. (1.3a) is not discussed further.

Since approximations to the distorted waves are central to the discussion here and calculations for proton-helium as well as proton-hydrogen collisions are presented, a symmetric form of the $B2$ amplitude is introduced, namely,

$$A_{B2}(E)=\tfrac{1}{2}(\langle X_f|V_{Pe}|\Phi_i\rangle+\langle\Phi_f|V_{Te}|X_i\rangle) , \quad (1.4)$$

which is equivalent to those listed in Eq. (1.1). In addition, it is convenient to separate explicitly the first Born term $A_{B1}(E)$ in Eq. (1.4) by working only with the scattered part of the distorted waves. Thus, $A_{B2}(E)$ is written as

$$A_{B2}(E)=\langle\Phi_f|V_{Pe}|\Phi_i\rangle+\tfrac{1}{2}(\langle\psi_f|V_{Pe}|\Phi_i\rangle+\langle\Phi_f|V_{Te}|\psi_i\rangle)$$

$$=A_{B1}(E)+A_2(E) , \quad (1.5)$$

where the partial amplitude $A_2(E)$ has been introduced and the scattered parts of the distorted waves are defined as

$$|\psi_i\rangle=G_0^+(E)V_{Pe}|\Phi_i\rangle , \quad (1.6a)$$

$$\langle\psi_f|=[G_0^-(E)V_{Te}|\Phi_f\rangle]^\dagger . \quad (1.6b)$$

Relaxing the terminology, these new states are also called distorted waves.

When the wave functions and potentials in Eq. (1.5) are transformed to momentum space, the discussion proceeds by showing that the exact amplitude is approximated well if certain limited regions of momentum space are emphasized. The ensuing forms for the distorted waves equations (1.6) then allow the calculation of simple closed-form expressions for the amplitude.

II. AMPLITUDE EVALUATION

Beginning with Eq. (1.5), a complete set of heavy-particle plane-wave states is inserted[15,16] between the distorted waves and the potential in the partial amplitude $A_2(E)$. This leads to the expression

$$A_2(E)=\tfrac{1}{2}\int d\mathbf{k}_i d\mathbf{k}_f[\tilde{\phi}_f^*(\mathbf{k}_f)\tilde{V}_{Te}(\mathbf{k}_i+\mathbf{J})\tilde{\psi}_i(\mathbf{k}_f,\mathbf{k}_i)+\tilde{\psi}_f^*(\mathbf{k}_i,\mathbf{k}_f)^*\tilde{V}_{Pe}(\mathbf{k}_f-\mathbf{K})\tilde{\phi}_i(\mathbf{k}_i)] , \quad (2.1)$$

where momentum-space versions of the distorted waves, Eqs. (1.6), are given by

$$\tilde{\psi}_i(\mathbf{k}_f,\mathbf{k}_i)=\tilde{G}_0^+(E)\tilde{V}_{Pe}(\mathbf{k}_f-\mathbf{K})\tilde{\phi}_i(\mathbf{k}_i) , \quad (2.2a)$$

$$\tilde{\psi}_f^*(\mathbf{k}_i,\mathbf{k}_f)=\tilde{\phi}_f^*(\mathbf{k}_f)\tilde{V}_{Te}(\mathbf{k}_i+\mathbf{J})\tilde{G}_0^+(E) . \quad (2.2b)$$

The free Green's function in momentum space assumes the form

$$\tilde{G}_0^+(E)=[(v^2/2+\mathbf{v}\cdot\mathbf{k}_f+\varepsilon_f)-(\mathbf{k}_i+\mathbf{k}_f-\mathbf{K})^2/2+i\eta]^{-1} . \quad (2.3)$$

A tilde on a function denotes Fourier transformation.

The heavy-particle part of the momentum transferred to the projectile in the collision is denoted by $\mathbf{K}$ and that transferred to the target nucleus by $\mathbf{J}$; momentum conservation is represented by the relation

$$\mathbf{K}+\mathbf{J}+\mathbf{v}=\mathbf{0} , \quad (2.4)$$

which is valid to order $1/M_P$ and $1/M_T$. The squared norm of $\mathbf{K}$ is given by $K^2=K_z^2+K_\perp^2$ with $K_z=-v/2-(\varepsilon_B+\varepsilon_f)/v$, and $K_\perp$ being the transverse momentum transfer; $\mathbf{K}_z$ is taken to be parallel to $\mathbf{v}$, the impact velocity vector. The experimental target binding energy ε_B and projectile bound-state energy ε_f are used in defining K_z. Equation (2.4) states that the outgoing momentum $\mathbf{v}$ of the captured electron is attained in the two collisions modeled by the $B2$ amplitude.

In the LPA version of Eq. (2.1), terms quadratic in $\mathbf{k}_i$ and $\mathbf{k}_f$ are neglected in Eq. (2.3) as are the $\mathbf{k}_i$ dependence of $\tilde{V}_{Te}(\mathbf{k}_i+\mathbf{J})$ and the $\mathbf{k}_f$ dependence of $\tilde{V}_{Pe}(\mathbf{k}_f-\mathbf{K})$. The momentum regions around the peaks of the wave functions—$\tilde{\phi}_i$ about $\mathbf{k}_i=0$ and $\tilde{\phi}_f$ about $\mathbf{k}_f=0$—are assumed to give the main contributions to the corresponding integrals.

For the MPA, Eq. (2.1) is evaluated by adding to the LPA contribution another part in each of the terms in $A_2(E)$. The distorted wave $\tilde{\psi}_f$ is approximated by neglecting the $\mathbf{k}_f$ dependence of $\tilde{V}_{Pe}$ and choosing the momentum of the initial bound state to be $\mathbf{J}$ while still treating the propagator exactly. The distorted wave $\tilde{\psi}_i$ is approximated analogously, taking the value $\mathbf{K}$ for the final-bound-state momentum, neglecting $\mathbf{k}_i$ in $\tilde{V}_{Te}$, but treating the propagator exactly.

Explicitly, the distorted waves are written

$$\tilde{\psi}_i(\mathbf{k}_f,\mathbf{k}_i)\approx\tilde{G}_0^+(E)\tilde{V}_{Pe}(\mathbf{K})\tilde{\phi}_i(\mathbf{J}) ,$$

$$\tilde{\psi}_f^*(\mathbf{k}_i,\mathbf{k}_f)\approx\tilde{\phi}_f^*(\mathbf{K})\tilde{V}_{Te}(\mathbf{J})\tilde{G}_0^+(E) .$$

The partial amplitude A_2^{MPA} is thus seen to be

$$A_2^{\mathrm{MPA}}=\tilde{V}_{Te}(\mathbf{J})\left[\int d\mathbf{k}_i d\mathbf{k}_f[\tilde{\phi}_f^*(\mathbf{k}_f)\tilde{G}_L^+(E)\tilde{\phi}_i(\mathbf{k}_i)\right]\tilde{V}_{Pe}(\mathbf{K})$$
$$+(\tfrac{1}{2})\left[\left[\int d\mathbf{k}_i d\mathbf{k}_f\tilde{\phi}_f^*(\mathbf{k}_f)\tilde{V}_{Te}(\mathbf{k}_i+\mathbf{J})\tilde{G}_0^+(E)\right]\tilde{V}_{Pe}(\mathbf{K})\tilde{\phi}_i(\mathbf{J})\right.$$
$$\left.+\tilde{\phi}_f^*(\mathbf{K})\tilde{V}_{Te}(\mathbf{J})\left[\int d\mathbf{k}_i d\mathbf{k}_f\tilde{G}_0^+(E)\tilde{V}_{Pe}(\mathbf{k}_f-\mathbf{K})\tilde{\phi}_i(\mathbf{k}_i)\right]\right] ,$$

which implicitly defines the integrals I_1, I_2, and I_3 through the equation

$$A_2^{\mathrm{MPA}}=\tilde{V}_{Te}(\mathbf{J})I_1\tilde{V}_{Pe}(\mathbf{K})+\tfrac{1}{2}[I_2\tilde{V}_{Pe}(\mathbf{K})\tilde{\phi}_i(\mathbf{J})+\tilde{\phi}_f^*(\mathbf{K})\tilde{V}_{Te}(\mathbf{J})I_3] . \quad (2.5)$$

The linearized, free Green's function is given by (new η)

$$\tilde{G}_L^+(E)=-2[K^2-v^2+Z_P^2+2(\mathbf{k}_f\cdot\mathbf{J}-\mathbf{k}_i\cdot\mathbf{K})-i\eta]^{-1}$$

when Eq. (2.4) is used and a 1s final state is assumed: $\varepsilon_f=-Z_P^2/2$.

Consideration of the integral I_3 in Eq. (2.5) shows that $\tilde{V}_{Pe}(\mathbf{k}_f-\mathbf{K})$ and $\tilde{G}_0^+(E)$ can peak simultaneously when $\mathbf{k}_i=0$ and $\mathbf{k}_f=\mathbf{K}$. It is precisely this fact that allows the significant contribution of the third term in the MPA amplitude. A similar conclusion can be shown to hold for the second term as well. In each case a particular large momentum component of the bound state is taken to evolve in the distorted wave while the electronic part of the momentum transfer in the potential transform of the wave is neglected. The propagator, which describes the evolution of the waves, is treated exactly.

The first term in Eq. (2.5) is easily evaluated for initial and final 1s states by first performing the angular integrations in combination with radial integrations by part. This is followed by use of Cauchy's residue theorem for the radial integral themselves.[4] Using the 1s momentum-space hydrogenic wave function for charge Z

$$\tilde{\phi}_{1s}(\mathbf{k})=2^{3/2}Z^{5/2}/\pi(k^2+Z^2)^2 , \quad (2.6)$$

the result is found to be

$$I_1=-(4\pi)^2(Z_PZ_T)^{3/2}/[K^2-v^2+Z_P^2-2i(Z_PJ+Z_TK)] . \quad (2.7)$$

Comparison of Eq. (2.7) with the definition of $\tilde{G}_L^+(E)$ shows that k_i and k_f have assumed the "average" values iZ_T and iZ_P, respectively, as Eq. (2.6) implies.

The second and third terms of Eq. (2.5) are formally identical for 1s states. Thus, only one of them, say I_3, needs to be considered here. Taking the potential transform $\tilde{V}_{Pe}(\mathbf{K})=-Z_P(2/\pi)^{1/2}/K^2$, and performing the angular integrations one has

$$I_3=-(2^3\pi^{1/2}Z_PZ_T^{5/2}/v)\int_0^\infty dk_i k_i\int_0^\infty dk_f k_f^{-2}\{[(k_i+k_f)^2+Z_T^2]^{-1}-[(k_i-k_f)^2+Z_T^2]^{-1}\}$$
$$\times\ln[(k_i^2+2k_fv+Z_T^2-i\eta)/(k_i^2-2k_fv+Z_T^2-i\eta)] .$$

Defining $u=2k_fv/(k_i^2+Z_T^2)$ and using the symmetry of the k_i integrand gives

$$I_3=-2^4\pi^{1/2}Z_PZ_T^{5/2}\int_0^\infty du\, u^{-2}\ln[(1+u-i\eta)/(1-u-i\eta)]$$
$$\times\int_{-\infty}^{+\infty}dk_i k_i(k_i^2+Z_T^2)^{-1}\{[k_i+(k_i^2+Z_T^2)u/2v]^2+Z_T^2\}^{-1} .$$

The k_i integration with use of the u integrand symmetry leads to

$$I_3=(2^4\pi^{3/2}Z_PZ_T^{3/2}/v)\int_{-\infty}^{+\infty}du\, u^{-1}\ln(1+u-i\eta)[1+(Z_Tu/v)^2]^{-2} ;$$

finally, performing the u integration one obtains the very simple form

$$I_3=i2^3\pi^{5/2}Z_PZ_T^{3/2}v^{-1}[2\ln(1-iv/Z_T)-(1+iZ_T/v)^{-1}] .$$

Expanding both terms in the square brackets of this equation as functions of Z_T/v one finds to order $(Z_T/v)^2$ the expression

$$I_3 = -i2^3\pi^{5/2}Z_P Z_T^{3/2} v^{-1}[2\ln(Z_T/v)+(1+i\pi)-3iZ_T/v] \ . \tag{2.8}$$

Note here that $(Z_T/v)^2$ terms have been neglected relative to the $\ln(Z_T/v)$ term. A similar result holds for I_2 but with Z_P and Z_T interchanged.

The MPA form of the A_2 amplitude is thus seen to be

$$\begin{aligned} A_2^{\text{MPA}}(E) = -[2^5\pi(Z_P Z_T)^{5/2}/(JK)^2]\{&[K^2-v^2+Z_P^2-2i(Z_P J+Z_T K)]^{-1} \\ &+i[Z_P K^2/2v(K^2+Z_P^2)^2][2\ln(Z_T/v)+(1+i\pi)-3iZ_T/v] \\ &+i[Z_T J^2/2v(J^2+Z_T^2)^2][2\ln(Z_P/v)+(1+i\pi)-3iZ_P/v]\} \ . \end{aligned} \tag{2.9}$$

The LPA version is

$$A_2^{\text{LPA}}(E) = -2^5\pi(Z_P Z_T)^{5/2}/\{(JK)^2[K^2-v^2+Z_P^2-2i(Z_P J+Z_T K)]\} \ . \tag{2.10}$$

Terms involving Z_P^2 and Z_T^2 are retained in Eqs. (2.9) and (2.10) in order to treat lower impact velocities better. Adding the partial amplitudes to A_{B1} gives

$$A_{B2}^{\text{MPA}}(E) = A_{B1}(E) + A_2^{\text{MPA}}(E) \ , \tag{2.11}$$

$$A_{B2}^{\text{LPA}}(E) = A_{B1}(E) + A_2^{\text{LPA}}(E) \ . \tag{2.12}$$

The first Born amplitude for 1s states is[12]

$$A_{B1}(E) = -2^5\pi(Z_P Z_T)^{5/2}/(K^2+Z_P^2)^3 \ .$$

In Sec. III results obtained using Eqs. (2.11) and (2.12) are compared with an exact evaluation of Eq. (2.1).

III. RESULTS AND DISCUSSION

A comparison of results derived from exact, MPA, and LPA evaluations of the $B2$ capture amplitude are given in this section in order to demonstrate explicitly that the exact amplitude is approximated well by the MPA version, at least for $1s \rightarrow 1s$ capture. Collisions of protons with hydrogen and helium atoms are considered. An effective charge Z_s of 1.6875 is used in the helium case.

In Figs. 1 and 2 differential cross sections derived from Eqs. (2.11) and (2.12) for the MPA and LPA, respectively, are compared with those obtained from exact numerical evaluations of Eq. (2.1) due to Simony and McGuire[8,17] for hydrogen and to Simony *et al.*[11] for helium. It is seen that the primary effect of the extra peaking terms present in the MPA is to give a much better representation of the exact cross section away from the Thomas-peak area which is centered around 0.054° in the hydrogen case and 0.034° in the helium case. The improvement of the MPA over the LPA is striking. Differences of factors of 2 or more between LPA and exact results have been reduced to percentages for the MPA results.

The poorest agreement is found in the vicinity of the local minimum of the cross sections where the largest cancellation among the various terms occurs and where one has, consequently, the most sensitive test of second-order terms. A better treatment of the free propagator in the amplitude in which some quadratic momentum terms are retained shows the local-minimum value to be raised, e.g., by 25% over the MPA value for 10-MeV proton-hydrogen collisions; however, a closed-form result is lost.[18]

The total cross section is obtained by integrating the amplitude squared over transverse momentum transfers:

$$\sigma = (2\pi v^2)^{-1}\int_0^\infty dK_\perp K_\perp |A|^2 \ .$$

The larger MPA differential cross sections seen in the extreme forward region $\theta \lesssim 0.01°$ in Figs. 1 and 2 are compensated for partially by their smaller values outside this region, implying that the total cross sections should agree better with the exact ones. This is indeed the case as Table I shows for both hydrogen and helium. At 500 keV and higher energies, MPA and exact values agree to better than 8%, with higher accuracy being attained as the impact energy is increased. It should appear from this trend that the exact value in the 50-MeV helium case is somewhat in error. This is quite possible because of the great difficulty of performing an exact calculation at high energy due to the sharp peaks in the momentum integrals.[17] Since the extreme forward angular region dominates the total cross section at lower energies, however, the larger values of the MPA cause it to fail relative to the exact result as the 100-keV values in Table I show.

Experimental total cross sections[19–23] are also shown in Table I. It is seen that the exact $B2$ cross sections differ considerably from the data, being generally too large. This poor agreement along with the good reproduction of the exact cross sections by the MPA ones which are derived by making use of the large bound-state momentum components implies that the second Born approximation suffers from the same deficiency as does the first Born approximation, namely, that high-momentum components play a disproportionate role in the collision process. Recent experimental differential[24] cross sections further support this idea.

As is well known,[2] the overall velocity dependence of the LPA total cross section is v^{-11} which follows as a re-

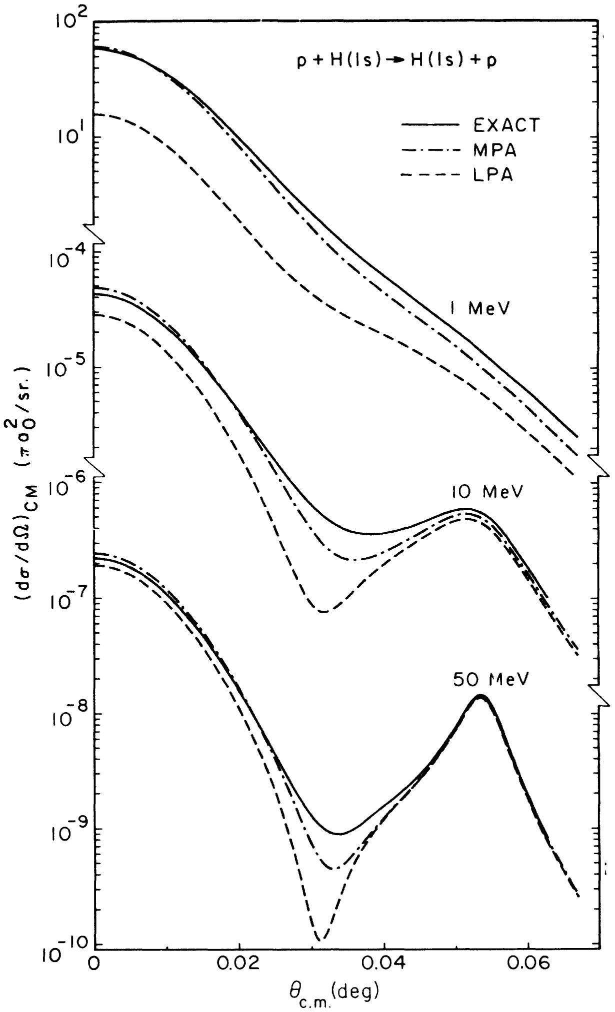

FIG. 1. Center-of-mass differential cross sections for $1s \rightarrow 1s$ capture in proton-hydrogen collisions. Results of calculations representing three levels of approximation to the second Born amplitude are shown: exact, —— (Ref. 8); multiple-peaking approximation (MPA), —·—·—· [Eq. (2.11)]; and linearized-propagator approximation (LPA), — — — [Eq. (2.12)].

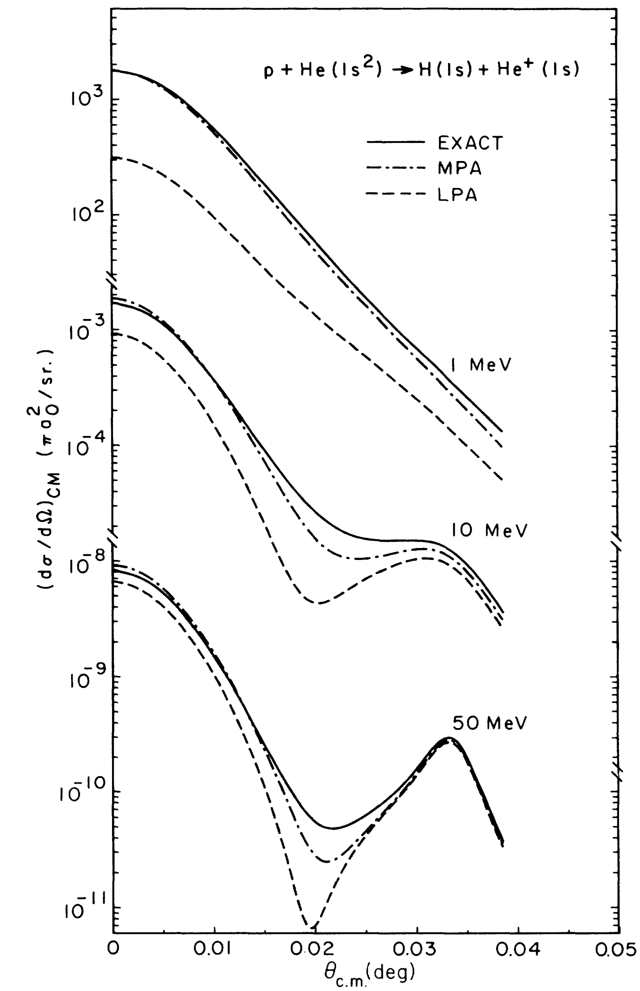

FIG. 2. Center-of-mass differential cross sections for $1s \rightarrow 1s$ capture in proton-helium collisions. Results of calculations representing three levels of approximation to the second Born amplitude are shown: exact, —— (Ref. 11); multiple-peaking approximation (MPA), —·—·—· [Eq. (2.11)]; and linearized-propagator approximation (LPA), — — — [Eq. (2.12)].

TABLE I. Comparison of approximate and exact second Born $1s \rightarrow 1s$ total capture cross sections (in units of πa_0^2/electron) vs impact energy E in MeV for protons on H and He. The numbers in square brackets are powers of 10.

	$p \rightarrow H$				$p \rightarrow He$			
E (MeV)	LPA	MPA	Exact[a]	Experiment[b]	LPA	MPA	Exact[c]	Experiment
0.1	8.76[−1]	3.47[0]	1.58[0]	1.4[−1][d]	1.02[+1]	2.11[+1]		3.1[−1][d]
0.2	2.16[−2]	1.15[−1]	9.13[−2]	1.0[−2]	2.04[−1]	7.51[−1]		4.0[−2]
0.5	1.53[−4]	7.53[−4]	7.95[−4]	5.6[−5][e]	1.40[−3]	7.60[−3]		1.2[−3][e]
1.0	3.18[−6]	1.25[−5]	1.36[−5]	2.3[−6][d]	3.24[−5]	1.60[−4]	1.74[−4]	5.6[−5]
3.0	5.52[−9]	1.45[−8]	1.50[−8]	2.7[−8][f,g]	6.58[−8]	2.22[−7]		1.4[−7][h]
5.0	2.76[−10]	6.05[−10]	6.09[−10]		3.40[−9]	9.42[−9]		1.0[−8][g]
7.0	3.81[−11]	7.49[−11]	7.41[−11]		4.76[−10]	1.16[−9]		
10.0	4.67[−12]	8.25[−12]	8.04[−12]		5.88[−11]	1.27[−10]	1.30[−10]	1.2[−10][i,g]
20.0	7.92[−14]	1.17[−13]			1.01[−12]	1.74[−12]	1.72[−12]	
50.0	3.61[−16]	4.53[−16]	4.51[−16]		4.89[−15]	6.69[−15]	6.25[−15]	

[a]McGuire (Ref. 17).
[b]Values are per H_2 molecule.
[c]Simony *et al.* (Ref. 11).
[d]Barnett and Reynolds (Ref. 19).
[e]Williams (Ref. 20).
[f]Schryber (Ref. 21).
[g]Interpolated value.
[h]Welsh *et al.* (Ref. 22).
[i]Barker *et al.* (Ref. 23).

sult of the term $K^2-v^2+Z_P^2$ in $\tilde{G}_L^+(E)$ passing through zero for a certain value of $K_\perp$. On the other hand, the first Born cross section is proportional to v^{-12}. Consideration of Eq. (2.9) shows the presence of a $(\ln v)/v$ factor in the MPA amplitude in addition to the other mentioned factors. Since $(\ln v/)v$ goes to zero for v going to infinity, the fundamental dominance of the LPA part is not altered, but how fast the large velocity limit is reached *is* affected. This fact coupled with the above-reported results then explains, to a large extent, the slow convergence of the exact cross section to the limiting dependence v^{-11}.

The present discussion also has particular relevance to a Faddeev-type theory of electron capture where an approximate evaluation of the amplitude is necessary due to the extreme difficulty of the numerical computations.[25] There, it can be shown that the contributions of the large-momentum components, which correspond to those contained in the MPA, are of the order $(Z_P/v)^2$ and $(Z_T/v)^2$ relative to the other terms in the amplitude. Such is clearly not the case for the MPA itself, as Eq. (2.9) shows. This partially explains then why the higher-order theory agrees better with experiment.[25]

In summary, use of a simple approximate analytic evaluation of the second Born capture amplitude (without internuclear contribution) has shown that the exact amplitude relies too heavily on the large momentum components of the initial and final bound states just as does the first Born approximation. It appears that a Faddeev-type approach to electron capture does not suffer from this problem. Additionally, a $\ln(v)/v$ correction to the velocity dependence of the total cross section is seen to be present which, although not of leading order, nevertheless slows convergence to the asymptotic v^{-11} form.

ACKNOWLEDGMENTS

I thank J. S. Briggs and the Universität Freiburg in the Federal Republic of Germany for their support when part of this work was carried out. Useful discussions with T. G. Winter are also acknowledged, as is his help with the manuscript.

[1]L. H. Thomas, Proc. R. Soc. London, Ser. A **114**, 561 (1927); R. Shakeshaft and L. Spruch, Rev. Mod. Phys. **51**, 369 (1979).

[2]R. M. Drisko, Ph.D. thesis, Carnegie Institute of Technology, 1955.

[3]K. Dettmann, in *Springer Tracts in Modern Physics* (Springer-Verlag, Berlin, 1971), p. 119.

[4]J. S. Briggs and L. J. Dubé, J. Phys. B **13**, 771 (1980); L. J. Dubé and J. S. Briggs, *ibid.* **14**, 4595 (1981).

[5]J. S. Briggs, Nucl. Instrum. Methods B **10/11**, 574 (1985); R. Shakeshaft and L. Spruch, Phys. Rev. A **29**, 605 (1984); K. Dettmann and G. Leibfried, Z. Phys. **218**, 1 (1969).

[6]P. J. Kramer, Phys. Rev. A **6**, 2125 (1972).

[7]J. E. Miraglia, R. D. Piacentini, R. D. Riverola, and A. Salin, J. Phys. **14**, L197 (1981).

[8]P. R. Simony and J. H. McGuire, J. Phys. B **14**, L737 (1981); P. R. Simony, Ph.D. thesis, Kansas State University, 1981.

[9]J. M. Wadehra, R. Shakeshaft, and J. H. Macek, J. Phys. B **14**, L767 (1981).

[10]J. H. McGuire, P. R. Simony, O. L. Weaver, and J. Macek, Phys. Rev. A **26**, 1109 (1982).

[11]P. R. Simony, J. H. McGuire, and J. Eichler, Phys. Rev. A **26**, 1337 (1982); J. H. McGuire, J. Eichler, and P. R. Simony, *ibid.* **28**, 2104 (1983).

[12]H. C. Brinkmann and H. A. Kramers, Proc. Acad. Sci. Amsterdam **33**, 973 (1930).

[13]S. Alston, in *Abstracts of Contributed Papers, Fourteenth International Conference on the Physics of Electronic and Atomic Collisions, Palo Alto, 1985*, edited by M. J. Coggiola, D. L. Huestis, and R. P. Saxon (North-Holland, Amsterdam, 1986), p. 517.

[14]C. J. Joachain, *Quantum Collision Theory* (North-Holland, Amsterdam, 1975).

[15]J. Macek and S. Alston, Phys. Rev. A **26**, 250 (1982).

[16]The transformations $\mathbf{R}_P=[M_P/(1+M_P)]\mathbf{R}_T+[(1+M_P+M_T)/(1+M_P)(1+M_T)]\mathbf{r}_T$ and $\mathbf{r}_P=[M_T/(1+M_T)]\mathbf{r}_T-\mathbf{R}_T$ are used in performing the heavy-particle integrations.

[17]J. H. McGuire (private communication).

[18]S. Alston (unpublished). The form of the propagator used is $\tilde{G}_0^+(E)\approx[(v^2-K^2-Z_P^2)/2+(\mathbf{k}_i\cdot\mathbf{K}-\mathbf{k}_f\cdot\mathbf{J})-(k_i^2+k_f^2)/2-i\eta]^{-1}$.

[19]C. F. Barnett and H. K. Reynolds, Phys. Rev. **109**, 355 (1958).

[20]J. F. Williams, Phys. Rev. **157**, 97 (1967).

[21]U. Schryber, Helv. Phys. Acta **40**, 1023 (1968).

[22]L. M. Welsh, K. H. Berkner, S. N. Kaplan, and R. V. Pyle, Phys. Rev. **158**, 85 (1967).

[23]K. H. Barker, S. N. Kaplan, G. A. Paulikas, and R. V. Pyle, Phys. Rev. **140**, A729 (1965).

[24]E. Horsdal-Pedersen, C. L. Cocke, and M. Stöckli, Phys. Rev. Lett. **50**, 1910 (1983); H. Vogt, R. Schuch, E. Justiniano, M. Schulz, and W. Schwab, *ibid.* **57**, 2256 (1986).

[25]S. Alston, in Ref. 13, p. 516; Phys. Rev. A (to be published).